Journal of Dynamic Behavior of Materials (2018) 4:211–221
https://doi.org/10.1007/s40870-018-0149-3

The Effects of Prior Cold Work on the Shock Response of Copper

J. C. F. Millett[1] · D. L. Higgins[2] · D. J. Chapman[3] · G. Whiteman[1] · I. P. Jones[2] · Y.-L. Chiu[2]

Received: 21 February 2018 / Accepted: 7 April 2018 / Published online: 24 April 2018

Abstract

A series of experiments have been performed to probe the effects of dislocation density on the shock response of copper. The shear strength immediately behind the shock front has been measured using embedded manganin stress gauges, whilst the post shock microstructural and mechanical response has been monitored via one-dimensional recovery experiments. Material in the half hard (high dislocation density) condition was shown to have both a higher shear strength and higher rate of change of shear strength with impact stress than its annealed (low dislocation density) counterpart. Microstructural analysis showed a much higher dislocation density in the half hard material compared to the annealed after shock loading, whilst post shock mechanical examination showed a significant degree of hardening in the annealed state with reduced, but still significant amount in the half hard state, thus showing a correlation between temporally resolved stress gauge measurements and post shock microstructural and mechanical properties.

Keywords Copper · Shock compression · Strength · Microstructure

Introduction

The response of metallic materials to external mechanical stimuli (including shock loading) is controlled by a number of factors at the microstructural level; type of unit cell, grain size, distribution and balance of additional phases and prior deformation history to name but a few. At the most fundamental level, it is probably the unit cell that has the greatest effect. Face centred cubic (FCC) metals such as copper, nickel or aluminium have been shown to deform via rapid dislocation motion, relaxing back to a dislocation cell structure on release [1–3]. The corresponding mechanical response under shock loading conditions involves a very low Hugoniot Elastic Limit (HEL—the yield strength under one-dimensional strain) and a fast (often exceeding the temporal resolution of the diagnostics) rise to the final shock amplitude [4]. Additionally, the shear strength has been observed to increase with time behind the shock front [5], and in the case of nickel at least, over near identical time scales for the shocked microstructure to reach its final confirmation [6]. In contrast, body centred cubic (BCC) metals such as tantalum have a higher and more clearly defined HEL and slower rise to the final shock amplitude [4, 7]. Shear strength was also shown to decrease behind the shock front [8]. It was suggested that this was due to the high Peierls stress characteristic of many BCC materials which reduced the ability of these materials to deform via dislocation generation, relying more on the motion of pre-existing dislocations, with transmission electron microscopy (TEM) of shocked tantalum showing that this was indeed the case [9]. However, the differences discussed above between FCC and BCC metals are an over simplification, with considerable variation occurring even within a single structural type. Reducing the stacking fault energy (SFE) in FCC metals, for example by alloying, can have a significant effect on the microstructural response. Rohatgi et al. [10–12] showed that alloying copper

✉ J. C. F. Millett
Jeremy.Millett@awe.co.uk

1 AWE, Aldermaston, Reading RG7 4PR, UK

2 School of Metallurgy and Materials Science, University of Birmingham, Elms Road, Edgbaston, Birmingham B15 2TT, UK

3 Institute of Shock Physics, Imperial College London, Prince Consort Road, South Kensington, London SW7 2AZ, UK

with aluminium up to 6 wt% induced a shift from rapid dislocation generation to a microstructure dominated by deformation twins. Similar effects have also been observed in low SFE materials such as austenitic stainless steels [13] and pure silver [14]. In mechanical terms, in austenitic stainless steel shear strength was observed to be largely constant behind the shock front [15], which was attributed to the increasing levels of twinning. Alternatively, changing the balance of additional phases within the microstructure has also been shown to have a strong effect. In the case of age hardened aluminium (Al 6061) and copper-beryllium alloys [16, 17], materials in the solution treated state displayed behaviour similar to that of pure aluminium or copper, a rapid rise of the shock front to the shock amplitude and an increase in shear strength behind the shock front. Aging the solution treated microstructure, thereby creating a distribution of fine, non-shearable particles throughout the microstructure, increased the rise time of the leading part of the shock, presumably by restricting the motion and generation of dislocations. Microstructural examination of Al 6061 [16] in the solution treated state showed a similar response to pure copper or nickel in that a dislocation cell structure was observed. This also corresponded to an increase in observed shear strength behind the shock front as well. Ageing the material resulted in a randomised dislocation distribution. The reduction in shear strength behind the shock front was also observed to be less.

Possibly the simplest way of modifying the mechanical response of a material is via cold working, thereby altering the density of dislocations present within the microstructure. In the case of tantalum, both quasi-isentropic loading [18] and shock loading [7, 19] has examined the effects of prior cold work. In annealed material, results showed that the elastic limit was clearly distinguishable, with an upper and lower yield point. Pre-rolling the material not only removed these upper and lower points, thus making the elastic limit more diffuse in nature, but reduced its magnitude as well. It was suggested in both reports that this was due to the presence of residual interstitial oxygen atoms accumulating around dislocations, effectively pinning them in position. Pre-rolling the tantalum would induce existing dislocations to move away from the surrounding oxygen atoms, hence resulting in a lower elastic limit.

The purpose of this paper is to provide further insights into the deformation of copper under plate impact loading conditions. Whilst the microstructural and mechanical response of copper to shock loading has been studied extensively (including the effects of residual strain [20], crystal orientation and pulse duration [21] and variations due to rise time in the loading pulse [3]), little work appears to have been done on the effects of the initial dislocation density on the shock response. In a previous paper, we examine this effect, by shock loading an as-received copper in a cold worked "half-hard" condition and comparing to the same material after an annealing treatment [22]. In this paper, we expand on that work by including shear strength measurements using laterally mounted stress gauges. The intention is to correlate the observed changes in the resultant microstructure and post shock mechanical response with the in situ strength measurements, thus increasing the understanding of the effects of initial dislocation density on the behaviour of copper during shock loading.

Experimental

Plate impact experiments have been performed on 100 mm diameter, 6 m and 70 mm, 3 m long smooth bore gas launchers. Target plates of copper 10 mm thick by 60 mm square (half hard) and 25 mm thick by 50 mm square (annealed) were sectioned in half and a manganin stress gauge (MicroMeasurements type J2M-SS-580SF-025) introduced 4 mm from the front surface. These particular gauges have been chosen as they have an active width of *ca*. 240 µm, thus giving a good temporal resolution. Due to their design, they are often referred to as 'T' gauges. The sample was re-assembled using a low viscosity epoxy adhesive with 25 µm of mylar on either side of the gauge for added protection. During curing, the sample was held in a special jig for a minimum of 12 h. After, the front surface was lapped to within five fringes from a monochromatic light source. This gauge was designed to measure the lateral component of stress (σ_y) and voltage–time data from the gauge output was converted to lateral stress using the methods of Rosenberg et al. [23] Since these gauges in both half hard and annealed copper were mounted at the same distance from the impact face, any differences in their response should be due to differences in materials behaviour rather than wave effects due to differing specimen geometry. A second stress gauge (MicroMeasurements type LM-SS-210DF-050/SP60) was supported on the front surface using a 2 mm thick copper coverplate. In this configuration, the gauge is sensitive to the longitudinal component of stress (σ_x), using the calibration of Rosenberg et al. [24]. From the output of these two gauges, the shear strength (τ) could be determined using the relation,

$$2\tau = \sigma_x - \sigma_y, \tag{1}$$

assuming the material is (near) isotropic. A schematic representation of the target assembly is shown in Fig. 1.

Shock stresses in the range 2.36–10.75 GPa were generated by the impact of 6 mm flyer plates made from either aluminium alloy 5082 or copper. It is clear from the target assembly schematic shown above that this technique is invasive, which have led some authors to question the validity of the gauge results [25]. However, laterally orientated stress gauges have been used successfully to measure shear strength in a wide variety of materials and the interested reader is directed to the review article by Millett [26] and the references therein.

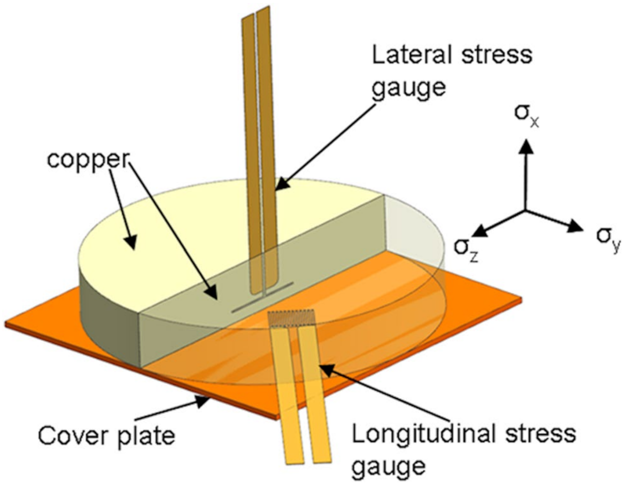

Fig. 1 Lateral stress gauge target assembly

A second series of experiments were performed to determine the microstructural response of copper to shock loading. 35 mm diameter by 5 mm thick disks of half hard and annealed copper were placed in target assemblies consisting of concentric rings of half hard copper and phosphor bronze to prevent lateral releases entering the specimen location. A series of 1 mm thick half hard copper disks were placed immediately behind the sample to prevent spallation effects occurring and finally a 1 mm copper coverplate was placed at the front surface of the target assembly to remove shear deformation effects at the impact face. These experiments were based on the methodology developed by Gray and co-authors [27–31] and photographs of a typical recovery target assembly are shown in Fig. 2. Shock stresses of 5.1, 5.9 and 9.6 GPa were induced by the impact of copper flyer plates at velocities of 275, 315 and 499 m s^{-1}. Flyer thicknesses were *ca*. 2.3 mm so as to provide a 1 µs pulse duration. Although the target design ensured that the specimen was loaded and unloaded purely under conditions of one-dimensional strain, the sample itself still had to be brought to rest in such a manner as to prevent subsequent damage during the recovery process. As such, the sample was decelerated into bags containing a hydrated mixture of sodium polyvinylacetate and wood pulp, which also quenched the samples back to ambient temperatures.

After the samples had been recovered, 3 mm disks were trepanned out and then twin jet polished using a solution of 33% nitric acid in methanol. Microstructures were observed via TEM using a JEOL 2100 with an accelerating voltage of 200 kV. Further details can be found in Higgins et al. [22, 32]. Mechanical testing on pre and post shocked samples was also performed on 5 mm diameter by 5 mm right cylinders, machined such that the long axis of the samples was parallel to the shock direction, in compression on a Zwick Roell Zmart. pro load frame at a strain-rate of 10^{-3} s^{-1}.

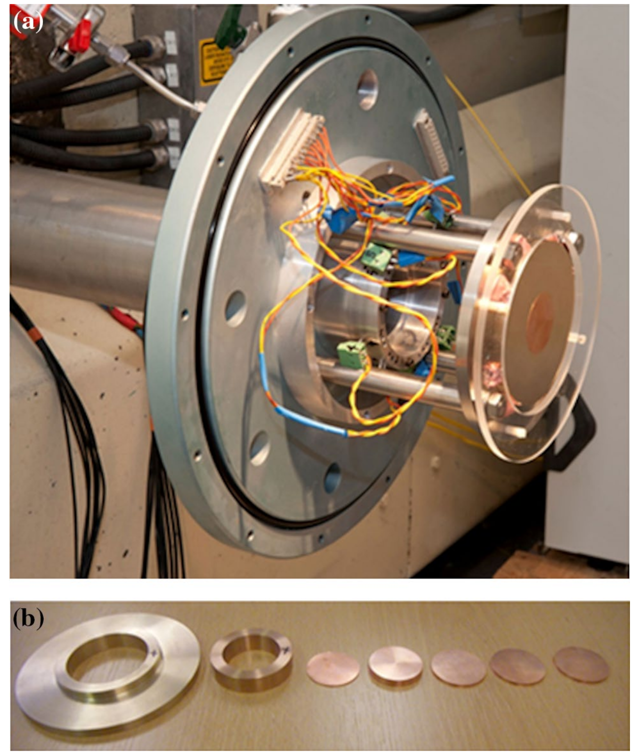

Fig. 2 Typical target assembly for a plate impact recovery experiment. **a** Complete assembly and **b** Disassembled target. The specimen is fourth from left

In both series of experiments, impact velocities were measured by Hetrodyne (photonic Doppler velocimetry—PDV) [33] velocimetry, using a 1550 nm laser.

Materials Data

Oxygen free, high conductivity copper was bought as 25 mm plate stock in the half hard condition, corresponding to an approximate reduction in thickness of 21%. The grain size was *ca*. 100 µm. To generate a low dislocation microstructure, the material was annealed at 425 °C for 1 h, followed by an air cool (Fig. 3).

The annealed material has a low dislocation density of *ca*. 3.8×10^8 cm^{-2}, and a grain size of *ca*. 64 µm. In contrast, the half hard material has a much higher dislocation density arranged in a cell network although it is near impossible to quantify. Acoustic and shock properties are presented below in Table 1.

Results

In Fig. 4, we present lateral stress gauge traces taken from an earlier investigation [35], in this case using stress gauges in a grid MicroMeasurements type (LM-SS-210DF-050/

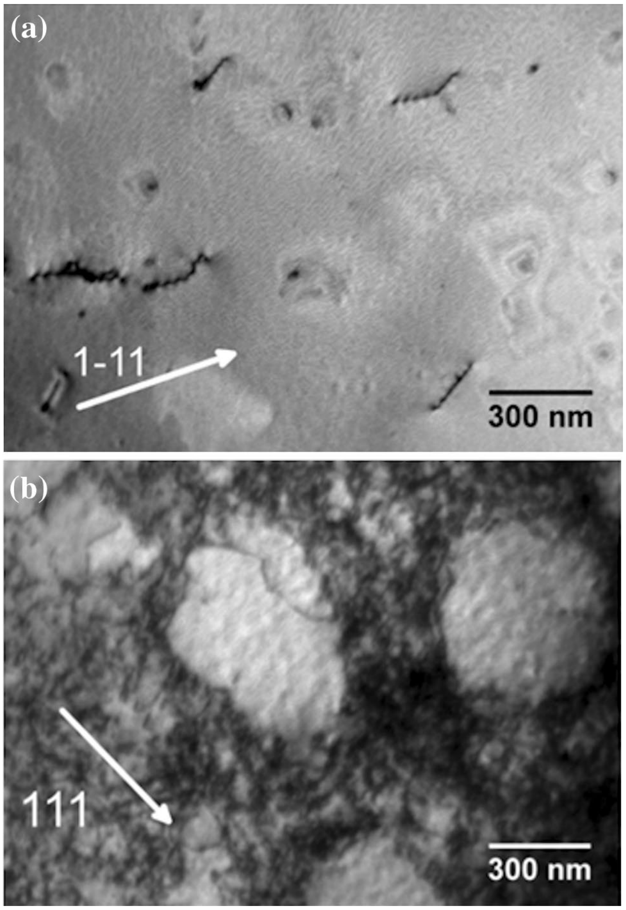

Fig. 3 Transmission electron micrographs of unshocked copper. **a** Annealed at 425 °C and **b** Half hard from the manufacturers

Table 1 Acoustic and shock properties of copper [34]

Longitudinal sound speed, c_L (mm μs^{-1})	4.76
Shear sound speed, c_S (mm μs^{-1})	2.33
Bulk sound speed, c_B (mm μs^{-1})	3.93
Density ρ_0 (g cm^{-3})	8.93
c_0 (mm μs^{-1})	3.94
S	1.49

The values c_0 and S are the shock parameters, taken from the relationship between shock velocity (U_S) and particle velocity (u_p), where $U_S = c_0 + Su_p$

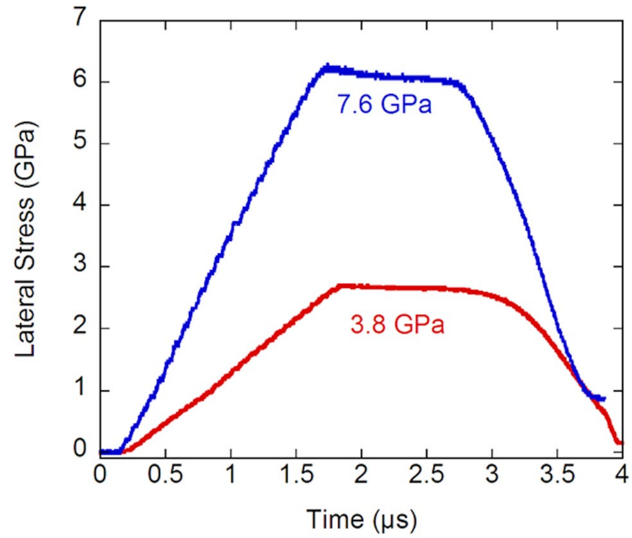

Fig. 4 Later stress gauge traces in annealed copper from a previous investigation [32]. Note that in this case, grid gauges (MicroMeasurements type LM-SS-210DF-050/SP60) were used rather than the 'T' gauge configuration used in more recent programmes

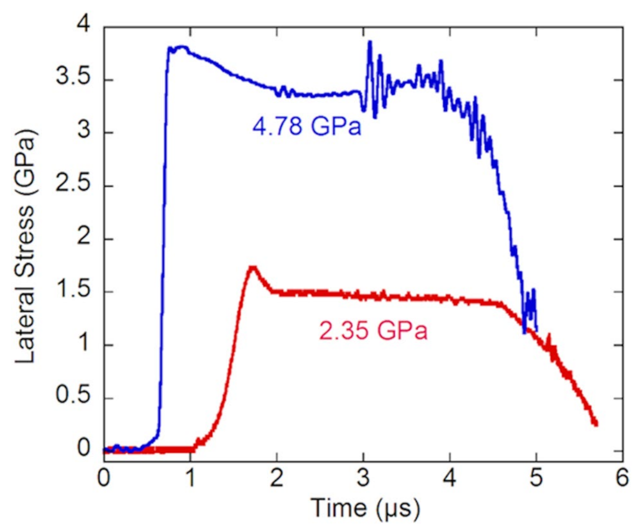

Fig. 5 Lateral stress gauge traces from as-received half-hard copper

SP60), rather than the more recent 'T' configuration. As a consequence, the rising part of the signal occurs over a period of *ca*. 1 μs as the shock front crosses the active width of the gauge. Indeed, as the shock crosses the gauge, each individual gauge element registers the shock, resulting in the step-like rise that is observed in each trace.

Once the stress front has passed over the entire gauge, the lateral stress would be expected to equilibrate once the Hugoniot stress has been reached. Note, however, there is a slight decrease in lateral stress behind the shock front. From Eq. 2 this suggests that the shear strength increases behind the shock front. However, due to the large scale of the gauge, there is a significant integrating effect that makes quantification of this shear strength near impossible. In Fig. 5, we present the equivalent results in half-hard copper, this time with laterally mounted stress gauges using the 'T' design.

Observe that the decrease in lateral stress behind the shock front noted in Fig. 4 is again present, although more pronounced. We believe that this is more an effect due to the greater temporal resolution of the 'T' gauge compared to the grid gauge, rather than inherent differences due to material's processing. However, these results are a strong indication that even in the half-hard state, copper can accommodate significant levels of dislocation generation during shock loading.

In Fig. 6, lateral stress data, in combination with the known longitudinal stress from the impact conditions, have been used to generate shear strength data, and its variation with longitudinal stress. This has been done for copper in both the annealed and rolled states, and we have also included similar data from Bat'kov et al. [36], also measured using lateral stress gauges, and McGonegle et al. [37] who used X-ray diffraction to measure changes in the lattice parameter during shock loading before using the results as input data into a molecular dynamics model to predict the shear strength.

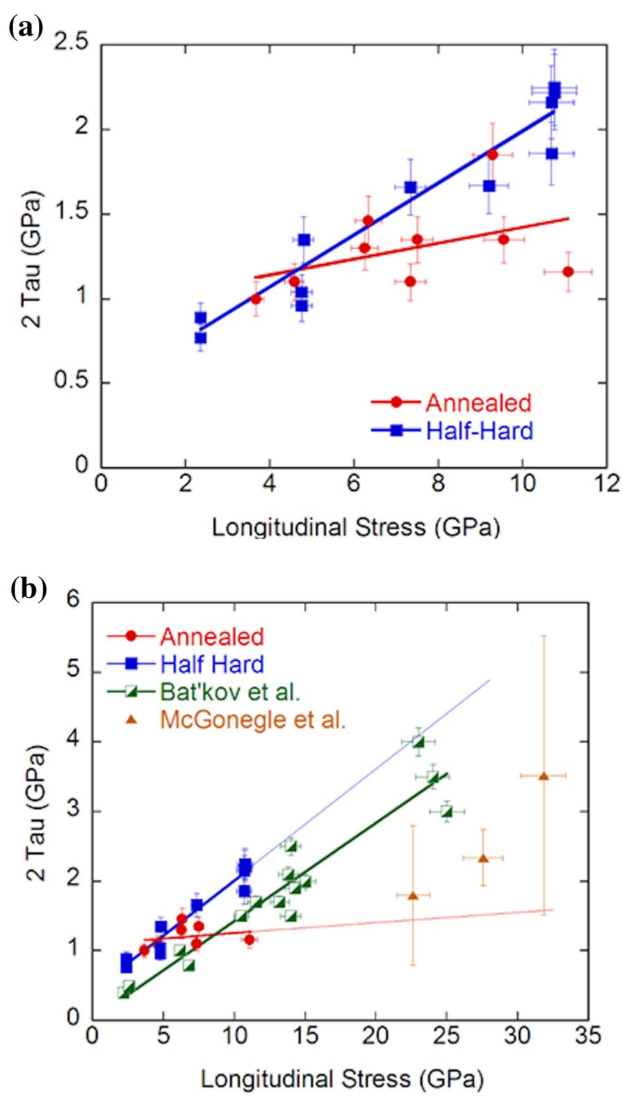

Fig. 6 Shear strength and its variation with longitudinal stress in annealed and rolled copper. **a** This investigation, **b** Comparison with the data of Bat'kov et al. [36] and McGonegle et al. [37]

It can be seen that the data lies on two separate trajectories, with the half hard material being more sensitive to impact stress than the annealed (Fig. 6a). We have expanded this in Fig. 6b by adding data from work by Bat'kov et al. [36] (using manganin stress gauges) and McGonegle et al. [37] (from X-ray diffraction measurements of lattice parameter in shock copper fed into a molecular dynamics model). Note that the data from Bat'kov et al. [36] although slightly lower than our own half hard data, follows pretty much the same gradient, suggesting that the material investigated here was also half hard. The data from McGonegle et al. [37] is broadly similar to all three data sets using gauges, even though this was made on laser shocked foils, diagnosed with X-ray diffraction. Clearly, the prior condition of copper has a strong effect upon its response to shock loading. This issue has been explored further in a series of experiments where samples of annealed and rolled copper have been shocked and recovered back to ambient, purely under conditions of one-dimensional strain. The results are shown in Fig. 7.

Both recovered microstructures have relaxed back into a cellular array of dislocations, typical of moderate to high SFE FCC metals such as copper [3] and nickel [1]. However, clear differences can be seen according to the material's initial starting condition. The annealed sample consists of well-defined dislocation cell walls, with relatively defect-free interiors. In contrast, in the rolled material, the cell walls are much thicker, with evidence of dislocations in the centres as well, indicating that the overall dislocation density after shocking is greater in the pre-rolled material.

In addition to examining the post shock microstructure, we have also investigated the post shock mechanical response as well. The results are presented in Fig. 8.

Note that the post shocked stress–strain curves have been displaced along the strain axes by the equivalent plastic strain due to the shock and release process, calculated the effective strain ($\varepsilon_{\mathrm{res}}$) from the relation [38],

$$\varepsilon_{res} = \frac{\sqrt{2}}{3}\left[\left(\varepsilon_x - \varepsilon_y\right)^2 + \left(\varepsilon_x - \varepsilon_z\right)^2 + \left(\varepsilon_y - \varepsilon_z\right)^2\right]^{\frac{1}{2}}, \qquad (2)$$

where the subscripts x applies to the loading axis and y and z lie in orthogonal directions. As the sample is under conditions of one-dimensional strain in the loading (x) direction, strain in the orthogonal directions (y and z) is zero, and thus Eq. 2 simplifies to,

$$\varepsilon_{res} = \frac{2}{3}\varepsilon_x. \qquad (3)$$

However, this only applies to the loading part of the complete shock cycle. If we assume that the equivalent strain is also imposed upon release, and that the true strain can be

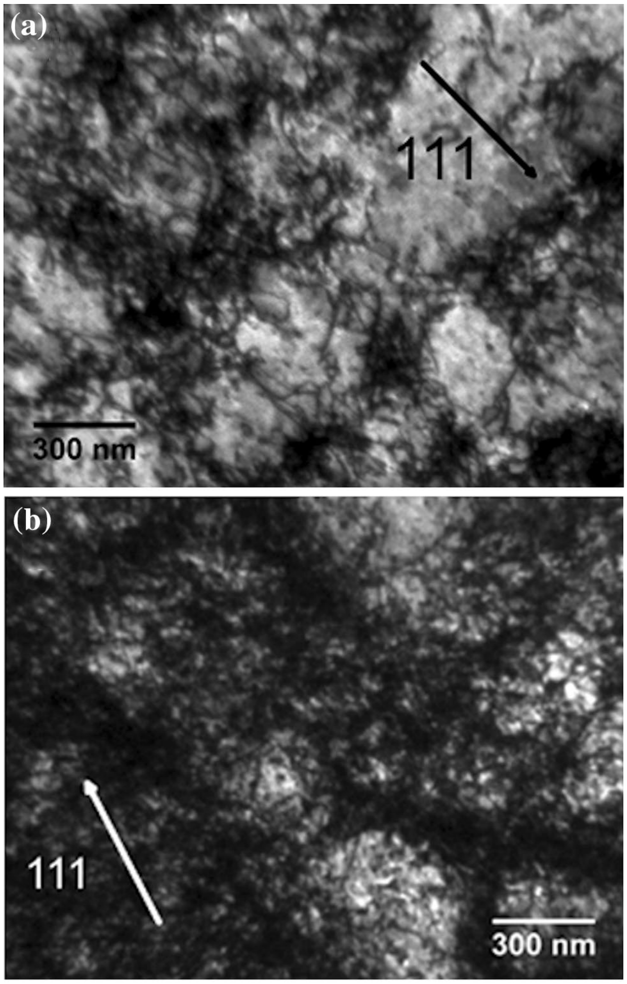

Fig. 7 Transmission electron micrographs of recovered copper after shock loading for 1 μs. **a** Annealed copper loaded to 5 GPa and **b** Half-hard copper loaded to 6 GPa

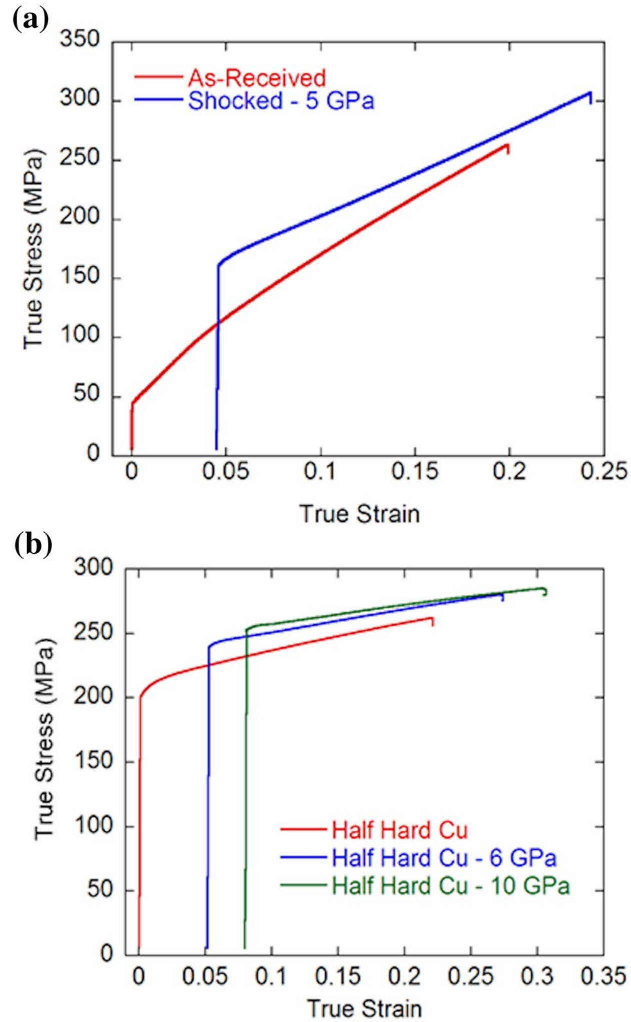

Fig. 8 Quasi-static mechanical response of shock loaded copper. **a** Annealed material shocked to 5 GPa and **b** Half-hard copper shocked to 6 and 10 GPa

expressed as the natural logarithm of the ratio of the shocked (V) and ambient specific volumes (V_0), the total equivalent strain imposed on shock and release becomes,

$$\varepsilon_{res} = \frac{4}{3} \ln \left[\frac{V}{V_0} \right]. \tag{4}$$

Results show that the response of copper to shock loading, as indicated by the microstructural results in Fig. 7, is strongly dependent upon the initial state prior to shock loading. The post shock mechanical response also displays a similar dependence. In the case of the annealed material (Fig. 8a), the shocked sample displays a significant degree of post shock hardening, and a reduced degree of work hardening. This is in agreement with recovery work performed by Gray and Morris [3] on copper, and in a wider context on high SFE FCC metals such as nickel and aluminium alloys [1, 16]. In its as-received, half hard state, the post shock stress–strain curves show a reduction in post shock hardening compared to the annealed state, but still significant. We also note that it appears that there is a slight and progressive reduction in work hardening as shock pressure increases.

Discussion

The results presented above show a clear effect of prior microstructure of copper, both from in situ shear strength measurements and post shock microstructural and mechanical property development. From Fig. 6a, it is clear that strength of copper in its half hard state increases more rapidly than in an annealed state. In Fig. 6b, we have included two further sets of data from the literature; lateral stress gauge data from Bat'kov et al. [36], and McGonegle et al. [37] from X-ray diffraction measurements of the lattice parameter during shock loading. The most obvious inference is that the half hard copper is stronger than the annealed material. Certainly at quasi-static strain-rates, as seen from Fig. 8, this is true, with annealed copper having a yield strength of *ca*. 50 MPa, whilst the half hard yields at *ca*. 200 MPa. Note however, that the data of Bat'kov et al. [36], whilst lying slightly lower than our own half hard data, appears to have the same rate of change of shear strength with longitudinal stress. In a previous article [35], it was suggested that these differences were due to the analysis routines used on the data gathered from the lateral stress gauges. Another (and more likely) possibility lies in the condition of the copper used in the Russian investigation. The authors cite the material as M1 copper. A search for the relevant properties has yielded incomplete results, but it has been noted that the material is supplied as either 'soft' or 'hard' cold-rolled. The suppliers have not specified the level of thickness reduction for either cold rolling process, further they report the resultant tensile stress strength but not the yield strength, which would be more useful for this investigation. Therefore, whilst it makes it difficult to draw a direct comparison between our own data and that of Bat'kov et al. [36], it would seem likely that the presence of a high initial dislocation density in their material has a significant effect on the in situ shock induced shear strengths, resulting in the higher sensitivity of shear strength to shock stress than in the annealed material. The situation with the data from McGonegle et al. [37] is less clear cut. The authors mention that it was purchased as 20 μm polycrystalline foil, which suggests that the material is also in a cold rolled condition, although no further information is given. Making this assumption, it would be expected that their results would be in agreement with those from our own half hard material, and from that of Bat'kov et al. [36], when in fact, they appear more consistent with the annealed material. The most likely reason for this lies in the differences in length and time scales used to load the samples. Bat'kov et al. [36] used an explosive loading system that resulted in a pulse duration between 1 and 3 μs, whilst McGonegle et al. [37] used a laser to shock load 20 μm foils for *ca*. 10 ns. Cao et al. [21] compared the microstructures of shocked single crystalline copper (in the <100> and <221> orientations), using either explosively driven flyer plates (pulse duration between 1.1 and 1.4 μs) or laser driven shocks of duration approximately 2.5 ns. They noticed significant differences between the two loading regimes, with regions of shear localisation in the plate impact loaded specimens that were completely absent from the laser loaded specimens. They attributed this to differences in heat transfer, which naturally took longer in the plate impact experiments, thus allowing greater thermal effects to manifest. From a wider perspective, Bourne [39] has pointed out that the deformation mechanisms available during a deformation event are influenced by the time available for deformation (i.e. shock pulse duration). In moderate to high SFE FCC metals such as copper or nickel, plastic deformation is generally controlled by the interaction between dislocations. However, this requires that mobile dislocations have to move over a distance before they interact, which will take time. Therefore, under very short pulse durations (such as those imposed by lasers), the time available does not allow significant dislocation interaction, and hence the strength characteristics of even a pre-shock work hardened material will, under these short pulse durations be more characteristic of a lower dislocation density at longer pulse durations. Note however, that the laser generated data, whilst starting in line with our annealed data, as stress increases, begins to trend towards the half hard results. This may be evidence that as shock stress increases, dislocation velocity also increases, thus reducing dislocation interaction times, making the strengthening observed more characteristic of a pre-cold rolled copper.

The microstructures from shock loaded copper in both the annealed and half hard states presented in Fig. 7 show dislocation cell structures. The annealed sample (shocked to 5 GPa) shows a cell structure typical of moderate to high SFE FCC metals such as copper and nickel. This is also an indication both that the sample was well aligned and that the momentum trapping rings kept residual lateral strains to a minimum. Gray et al. [20] demonstrated that as long as residual strains were $<2\%$, a cell structure would form. At 7%, a mixture of dislocation cells and planar dislocation arrays was observed, and heavy twin formation was noted at a residual strain of *ca*. 26%. Therefore we can be confident that there were no adverse lateral strain effects. The half hard sample (shocked to 6 GPa) also had a dislocation cell structure, but it can be seen that the cell walls are much thicker, and that there are dislocations present within the interiors. In simplistic terms this would appear reasonable; the higher population of dislocations in the rolled material would act as an increased source of extra dislocations during loading. However, there is relatively little work in the literature on the effects of prior deformation on the shock response of materials. The majority of this has concentrated on samples receiving repeat shock loading after recovery (see for example Gray and Huang [2] on pure aluminium or Moin and Murr [40] on nickel and 304 stainless steel). In the case of nickel [40], three consecutive loadings at 15 GPa (duration of 2 μs for each loading event) showed that cell walls were more defined (in other words a greater dislocation density) and the cells themselves were smaller than for a single load cycle. However, it was also noted that the cell dimensions were not equivalent to either a single loading event at 45 GPa for either 2 or 6 μs, with the cell size being larger in the repeat loadings than in either 45 GPa single events. This led the authors to suggest dislocation generation decreased with each subsequent loading cycle.

This would appear to be consistent with the quasi-static pre and post shock compression curves shown in Fig. 8. In the case of the annealed sample, once the strain imposed by the shock and release cycle has been accounted for, a considerable degree of hardening has occurred, although the level of work hardening has been reduced. This behaviour is consistent with a number of FCC metals including copper [3, 11], nickel [1] and some aluminium alloys [16, 41]. The most likely cause at the very high strain-rates occurring during shock loading, the mobility of dislocations are restricted, and thus to accommodate the strain imposed during shock loading, extra dislocations have to be generated. Consequently the quasi-static response of the shocked material, once the imposed shock strain has been accounted for will show a significant degree of post shock hardening, as can be seen in Fig. 8. With the half hard material, after again taking into account the strain imposed by shock and release, post shock hardening is again observed, but this time at a reduced level when compared to the same situation in the annealed material. This demonstrates that the material is still able to accommodate plastic deformation via dislocation generation, and is consistent with the increased dislocation density observed in the shocked microstructures shown in Fig. 7. This is also consistent with lateral stress traces from the half-hard material in Fig. 5 which show a reduction in lateral stress behind the shock front, suggesting that a level of hardening and hence dislocation generation is still occurring. We also note that the grain sizes between the annealed material (*ca*. 64 µm) and half hard (*ca*. 100 µm) are different and thus cannot be dismissed. However, we believe that the effect of grain size in these circumstances will be minimal for the following reasons. Firstly, whilst copper, like all FCC metals does have a grain size dependent yield strength (the Hall–Petch relationship), the sensitivity of strength to grain size is not great due to the relative ease in which new dislocations can be generated during deformation [38]. Given that the grain sizes in these two materials are not radically different, it would therefore be expected that grain size effects would not be large. Secondly, due to the ease of dislocation motion in copper during shock loading, the average dislocation interaction distance (in the case of nickel, which behaves in a similar way to copper, Bourne et al. estimated this to be of the order 170 nm [4]) is much less than the grain size, and thus under the extremely high loading rates experienced during shock loading, dislocations in copper won't have time to be influenced by grain boundaries. However, it is interesting to speculate if this would apply in nano-grained materials, although this is beyond the scope of this paper.

Finally, in Fig. 9, we present again the quasi-static stress strain curves from both the as-received and shocked conditions, this time including the strain imposed by the rolling process in the manufacture of the half hard material. This has been calculated from Eq. 2, based on the assumption

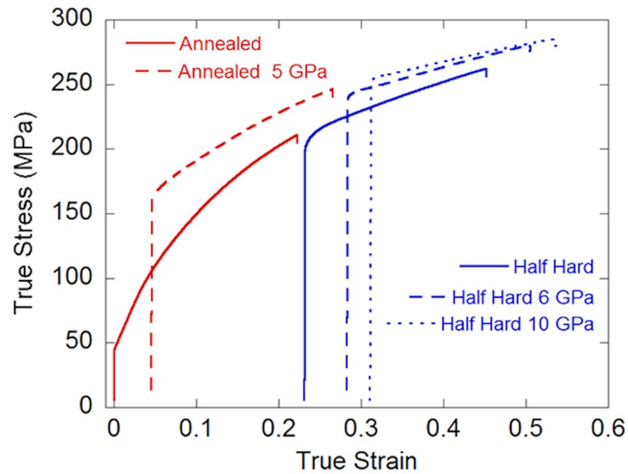

Fig. 9 Quasi-static stress-strain curves for annealed and half-hard copper, pre- and post shock. Note that in this figure, all pre-strain, including that imposed by the rolling process has been accounted for

that the material has been strip rolled (i.e. the rolling direction has been constant). Therefore, if strain in the z direction (width) is zero, then the equivalent strain in the through thickness (x) direction reduces to,

$$\varepsilon_{eq} = \frac{2}{\sqrt{3}} \ln\left[\frac{w}{w_0}\right], \tag{5}$$

where w_0 and w are the original and final thicknesses of the rolled material. Half-hard copper generally corresponds to a reduction in thickness of 21%, giving a true strain of 0.235. Two features are immediately obvious from this figure. Firstly, the stress–strain curve (accounting for the equivalent strain from the rolling) from the unshocked half hard material appears to be an extension of the annealed material. Given that copper (like most moderate to high SFE FCC metals) is a path dependent material, this implies that the imposed strain-rate during the rolling process is near identical to the strain-rate imposed during the quasi-static ($10^{-3}\ s^{-1}$) testing. It is interesting to note that this behaviour applies even though the copper in this investigation started in the half hard state with annealing from there rather than rolling from an initial annealed condition.

Similar behaviour can be observed in the quasi-static response of the shock recovered samples, with the half hard response lying on a (near) extension of the annealed material. However, it can be seen that the stress–strain curves of the pre-shocked half hard material do not quite correlate with the corresponding curve from the pre-shocked annealed copper. Specifically, it would appear that the curve from the half hard copper loaded to 6 GPa would lie slightly below that of the annealed sample shocked to 5 GPa, whilst the half hard 10 GPa curve does seem to be an extension of the annealed 5 GPa curve. We believe that this again is due to the path dependence of copper, specifically during the initial rise of the shock pulse. A reasonable estimate of the strain-rate imposed in the rise of the shock front can be determined using the methods of Grady [42] where the strain-rate ($\dot{\varepsilon}$) is related to the stress jump, σ (the difference in stress between the HEL and the final stress amplitude) via the relation,

$$\dot{\varepsilon} = A\sigma^4, \tag{6}$$

where A is a constant, although very recently we have presented evidence that it is an indication of dislocation mobility [43, 44] during shock loading. Using this approach, we can give a reasonable estimate of strain-rate at the shock levels in the recovery experiments discussed above; thus at 6 GPa, the strain-rate in the shock front is of the order $9.7 \times 10^6\ \mathrm{s}^{-1}$, whilst at 10 GPa, this is nearly an order of magnitude higher at $75 \times 10^6\ \mathrm{s}^{-1}$. This therefore suggests that the recovered sample from the 10 GPa shock should show a slightly higher quasi-static response than the sample recovered from 6 GPa. This approach can also provide an explanation of the differences between the quasi-static responses of the annealed and half hard coppers (after shock loading), with the annealed appearing slightly stronger. We would suggest that the higher initial dislocation density in the half hard material would reduce the mobility of those dislocations (compared to the fewer dislocations present in the annealed material), thus somewhat reducing the strain-rate in the shock front itself, with the result that the hardening due to the shock would be reduced by a small but finite amount. On a grosser scale, such differences in strain-rate due to changes in dislocation mobility have been observed in two different BCC metals [43], with niobium having a greater shock induced strain-rate than molybdenum due to the lower Peierls stress yielding an increase in dislocation mobility.

Conclusions

The effects of prior cold work on the shock response of copper have been investigated using stress gauges to determine the in situ shear strength and one-dimensional recovery to obtain the post shock microstructural and mechanical response. In the as-received, half hard condition (corresponding to a reduction in thickness via cold rolling of *ca*. 21%), the in situ shear strength and its change with increasing shock stress were shown to be greater than the corresponding change in the annealed state. These results (in the case of the half hard condition) are similar to those of previous workers where similar experiments were also performed on copper with prior cold work. We have suggested that the greater starting dislocation density in the half hard condition acts as an increased source of dislocations during shock deformation. We have noted with interest that the shear strengths generated during laser shock loading of (presumably) cold rolled copper foil are more consistent with our own results from annealed copper. We have suggested that this is due to the effects of the corresponding pulse durations. In the laser shock experiments, a pulse duration of *ca*. 10 ns was observed, compared to several microseconds in the case of plate impact. In the case of copper under shock loading conditions, the strength is controlled by the motion and interaction of dislocations. In the case of the laser loaded specimens, even though the dislocation density was high, the loading would be of sufficiently short duration that dislocation interactions would be minimal, thus giving a shear strength more akin to that of an annealed material. It is interesting to note, however, that as stress increases, the shear strength in these samples begins to increase towards that of our half hard material. We have assumed that this is due to the increasing dislocation velocity reducing the dislocation interaction times (and increasing dislocation interactions), hence resulting in a more rapid increase in strength.

Recovery experiments showed that in both the half hard and annealed states, the resultant shocked microstructure consisted of a well developed network of dislocation cells. This was consistent with previous studies of FCC materials with moderate to high stacking fault energies. It was observed however, that the cell walls in the half hard material were considerably higher than in their annealed counterparts. The corresponding quasi-static compression tests on shock loaded material showed that the annealed copper displayed a significant degree of post shock hardening (when compared to the unshocked response) but with a reduced degree of work hardening. We believe that this is due to the very high strain-rates encountered during shock loading resulting in a somewhat reduced dislocation mobility, thus requiring a higher degree of dislocation generation to accommodate the equivalent strain. Thus the higher dislocation density after shock loading results in a reduced work hardening post shock. With the copper in the half-hard condition, the level of post shock hardening is reduced, but still present, as suggested by the increased dislocation density in the cell walls observed in the TEM micrographs. Taking all the equivalent strains from both the rolling process and shock loading into account, a number of features have become prominent. Firstly, the quasi-static curve of the half-hard copper lies on an extension of that of the annealed material, implying that the strain-rate experienced during cold rolling was nearly identical to that imposed by the quasi-static upset tests themselves. Secondly, the quasi-static stress–strain response of the pre-shocked copper from both initial starting conditions also lie on or near the same quasi-static stress–strain curve. However, the precise nature of the shocked quasi-static response appears to have a small dependence on the shock amplitude, with the yield stress increasing slightly. We have suggested that this is due to variations in strain-rate in the shock front itself. We believe that increasing pre-shock dislocation density (i.e. the half hard material) reduces the overall dislocation mobility and hence reduces by a small yet significant degree the resultant strain-rate. In contrast, increasing the shock amplitude will increase the overall strain-rate, and hence the level of post shock hardening as well.

Acknowledgements We would like to thank Steve Johnson of Imperial College for providing technical support and gas gun operation. We would also like to thank Mike Lowe of AWE plc for his help with the shots and Simon Case (AWE plc) for his interest and encouragement. Finally, we are grateful to Dr. Bo Pang of the University of Birmingham for his assistance with the microstructural analysis.

References

1. Follensbee PS, Gray GT III (1991) The response of single crystal and polycrystal nickel to quasistatic and shock deformation. Int J Plast 7:651–660
2. Gray GT III, Huang JC (1991) Influence of repeated shock loading on the substructure evolution of 99.99 wt% aluminum. Mater Sci Eng A 145:21–35
3. Gray GT III, Morris CE (1991) Influence of loading paths on the mechanical response and substructure evolution of shock loaded copper. Journal de Physique IV Colloque C3:191–196
4. Bourne NK, Gray GT III, Millett JCF (2009) On the shock response of cubic metals. J Appl Phys 106:091301
5. Millett JCF, Bourne NK, Gray GT III (2008) The behaviour of nickel, Ni-60Co and Ni_3Al during one-dimensional shock loading. Metall Mater Trans A 39A:322–334
6. Murr LE, Kuhlmann-Wilsdorf D (1978) Experimental and theoretical observations on the relationship between dislocation cell size, density, residual hardness, peak pressure and pulse duration in shock-loaded nickel. Acta Metall 26:847–857
7. Millett JCF, Whiteman G, Park NT, Case S, Bourne NK (2013) The role of cold work on the shock response of tantalum. J Appl Phys 113:233502
8. Millett JCF, Bourne NK, Park NT, Whiteman G, Gray GT III (2011) On the behaviour of body centred cubic metals to one-dimensional shock loading. J Mater Sci 46:3899–3906
9. Gray GT III, Vecchio KS (1995) Influence of peak pressure and temperature on the structure /property response of shock-loaded Ta and Ta-10W. Metall Mater Trans A 26A:2555–2563
10. Rohatgi A, Vecchio KS (2002) The variation of dislocation density as a function of the stacking fault energy in shock-deformed FCC materials. Mater Sci Eng A 328:256–266
11. Rohatgi A, Vecchio KS, Gray GT III (2001) The influence of stacking fault energy on the mechanical behavior of Cu and Cu-Al alloys: deformation twinning, work hardening and dynamic recovery. Metall Mater Trans A 32A:135–145
12. Rohatgi A, Vecchio KS, Gray GT III (2001) A metallographic and quantitative analysis of the influence of stacking fault energy on shock hardening in Cu and Cu-Al alloys. Acta Mater 49:427–438
13. Xue Q, Gray GT III, Henrie BL, Maloy SA, Chen SR (2005) Infulence of shock prestraining on the formation of shear localization in 304 stainless steel. Metall Mater Trans A 36:1471–1486
14. Huang JC, Gray GT III (1988) Microstructural characterisation of Ag shock-loaded at high pressure. Scr Metall 22:545–550
15. Millett JCF, Whiteman G, Bourne NK (2009) Lateral stress and shear strength behind the shock front in three face centred cubic metals. J Appl Phys 105:033515
16. Millett JCF, Bourne NK, Chu MQ, Jones IP, Gray GT III, Appleby-Thomas G (2010) The role of aging on the mechanical and microstructural response of aluminum 6061 to one-dimensional shock loading. J Appl Phys 108:073502
17. Millett JCF (2015) Modifications of the shock response of materials by age hardening. Mater Trans A 46A:4506–4517
18. Asay JR, Ao T, Vogler TJ, Davis J-P, Gray GT III (2009) Yield strength of tantalum for shockless compression to 18 GPa. J Appl Phys 106:073515
19. Florando JN, El-Dasher BS, Chen C, Swift DC, Barton NR, McNaney JM, Ramesh KT, Hemker KJ, Kumar M (2016) Effect of strain rate and dislocation density on the twinning behavior in tantalum. AIP Adv 6:045120
20. Gray GT III, Follensbee PS, Frantz CE (1989) Effect of residual strain on the substructure development and mechanical response of shock-loaded copper. Mater Sci Eng A 111:9–16
21. Cao BY, Lassila DH, Schneider MS, Kad BK, Huang CX, Xu YB, Kalantar DH, Remington BA, Meyers MA (2005) Effect of shock compression method on the defect substructure in monocrystalline copper. Mater Sci Eng A 409:270–281
22. Higgins DL, Pang B, Millett JCF, Whiteman G, Jones IP, Chiu Y-L (2015) Contrasting the microstructural and mechanical response to shock loading of cold-rolled copper with annealed copper. Metall Mater Trans A 45A:4518–4521
23. Rosenberg Z, Bourne NK, Millett JCF (2007) On the effect of manganin geometries upon their response to lateral stress. Meas Sci Technol 18:1843–1847
24. Rosenberg Z, Yaziv D, Partom Y (1980) Calibration of foil-like manganin gauges in planar shock wave experiments. J Appl Phys 51:3702–3705
25. Winter RE, Harris EJ (2008) Simulations of embedded lateral stress gauge profiles in shocked targets. J Phys D 41:035503
26. Millett JCF (2017) Shear strength measurements during shock loading using laterally mounted stress gauges. AIP Conf Proc 1793:110015
27. Gray GT III (1990) Shock recovery experiments: an assessment. In: Schmidt SC, Johnson JN, Davison LW (eds) Shock compression of condensed matter—1989. North-Holland, Amsterdam, pp 407–414
28. Gray GT III (1991) Deformation substructures induced by high rate deformation. In: Lowe TC, Rollett AD, Follansbee PS, Daehn GS (eds) Modelling the deformation of crystalline solids. The Minerals, Metals and Materials Society, Warrendale, pp 145–158
29. Gray GT III (1991) Influence of shock-wave deformation on the structure/property behaviour of materials. In: Asay JR, Shahinpoor M (eds) High-pressure shock compression of solids. Springer, New York, pp 187–215
30. Gray GT III (1992) Shock experiments in metals and ceramics. In: Meyers MA, Murr LE, Staudhammer KP (eds) Shock-wave and high-strain-rate phenomena in materials. Marcel Dekker, New York, pp 899–911
31. Bourne NK, Gray GT III (2005) Computational design of recovery experiments for ductile metals. Proc R Soc A 461:3297–3312
32. Higgins DL (2017) High strain rate deformation of copper, titanium 6Al-4V and tantalum and quasi-static compression of tantalum. School of Metallurgy and Materials Science, University of Birmingham
33. Strand OT, Goosman DR, Martinez C, Whitworth TL, Kuhlow WW (2006) Compact system for high-speed velocimetry using hetrodyne techniques. Rev Sci Instrum 77:083108

34. Marsh SP (1980) LASL Shock Hugoniot data University of California Press Los Angeles
35. Millett JCF, Bourne NK, Rosenberg Z (1997) Shear stress measurements in copper, iron and mild steel under shock loading conditions. J Appl Phys 81:2579–2583
36. Bat'kov YV, Glushak BL, Novikov SA (1988) Strength of aluminum, copper and steel at front of shock wave. Combust Explos Shock Waves 25:635–640
37. McGonegle D, Higginbotham A, Galtier E, McBride EE, McMahon MI, Milathianaki D, Lee HJ, Nagler B, Vinko SM, Wark JS (2014) Investigations into rapid uniaxial compression of polycrystalline targets using femtosecond X-ray diffraction. J Phys 500:112063
38. Smallman RE (1985) Modern physical metallurgy. Butterworths, London
39. Bourne NK (2011) Materials' physics in extremes: akrology. Metall Mater Trans A 42A:2975–2984
40. Moin E, Murr LE (1979) Interactive effects of shock loading parameters on the substructure and mechanical properties of nickel and stainless steel. Mater Sci Eng 37:249–269
41. Gray GT III (1988) Deformation twinning in Al-4.8 wt%Mg. Acta Metall 36:1745–1754
42. Grady DE (2010) Structured shock waves and the fourth-power law. J Appl Phys 107:013506
43. Millett JCF, Cotton M, Bourne NK, Park NT, Whiteman G (2014) The behaviour of niobium and molybdenum during uni-axial strain loading. J Appl Phys 115:073506
44. Whiteman G, Keightley PT, Millett JCF (2016) The behaviour of 2169 steel under uniaxial stress and uniaxial strain loading. J Dyn Behav Mater 2:337–346